

Simultaneous Determination and Speciation of Zinc, Cadmium, Lead, and Copper in Natural Water with Minimum Handling and Artifacts, by Voltammetry on a Gel-Integrated Microelectrode Array

Jianhong Pei, Mary-Lou Tercier-Waeber, and Jacques Buffle*

CABE, Department of Inorganic, Analytical and Applied Chemistry, Science II, University of Geneva, 30 Quai E.-Ansermet, CH-1211 Geneva 4, Switzerland

The paper reports a new approach based on a gel-integrated Hg-plated-Ir-based microelectrode array (GIME), for measuring Cu, Pb, Cd, and Zn speciation in natural waters. This paper focuses on the quantitative discrimination between mobile and colloidal metal species (size limit of a few nanometers), for which most classical separation techniques present severe drawbacks. Previous papers have shown qualitatively that GIME combined with square wave anodic stripping voltammetry (SWASV) has the basic characteristics required to discriminate between these two fractions directly on the unperturbed sample. In addition, because of the large sensitivity provided by GIME, complexation parameters (equilibrium constants and site concentrations) can be determined in little-perturbed samples, particularly without metal addition or with small addition compared with natural concentrations. The advantages of this procedure are exemplified and the possible artifacts occurring when titrating the sample with metals, in particular intermetallic compound formation and other problems, are discussed in detail. The present paper shows that the characteristics of GIME make it a unique tool to get quantitative information on metal speciation at nanomolar or even subnanomolar levels, with only minor sample handling.

It is well-known^{1–5} that trace metal speciation (see glossary for the definition used in this paper) drastically influences metal circulation and bioavailability in aquatic media. The development of routine and, therefore, simple, cheap, and easily handled procedures for continuous, real time, preferably in situ trace metal monitoring and speciation in waters is thus highly needed for

quality assessment. It has been shown^{6–9} that microsensors coupled to voltammetric techniques are well-suited for this purpose. They are among the most sensitive techniques, and they enable the simultaneous determination of several elements, as well as species discrimination in low- or high-ionic-strength waters without or with minimum sample modification.^{7,10–14} In particular, it has been shown that gel-integrated microelectrodes (GIME), such as an agarose-gel-covered Hg-coated-Ir-based microelectrode or agarose-gel-covered Hg-coated-Ir-based microelectrode array,^{7,8,13,16} prevent the microelectrode from being fouled by natural colloids and biopolymers, usually encountered in real samples,^{1,17} while discriminating between colloidal species (larger than a few nanometers), on one hand, and the sum of free metal ions and metal complexes which are both labile and mobile (size of less than a few nanometers), on the other hand. Under the conditions used here, all mobile complexes are labile (see below), so that these complexes plus free metal ions will only be referred to as mobile species hereafter. The capability of GIME to discriminate between mobile and colloidal species is unique. All other procedures for discriminating between mobile and colloidal species at the nanometer size level make use of time-consuming techniques, like ultrafiltration, ultracentrifugation, or chromatography, which are prone to severe artifacts, when studying speciation at nanomolar or subnanomolar concentrations.

* Corresponding author: (fax) 41-22-702-6069; (e-mail) Buffle@CABE.UNIGE.CH.

- (1) Buffle, J. *Complexation Reactions in Aquatic Systems: An Analytical Approach*; Ellis Horwood: Chichester, U.K., 1988.
- (2) Stumm, W.; Morgan, J. J. *Aquatic Chemistry*; John Wiley & Sons: New York, 1981.
- (3) Tack, F. M. G.; Verloo, M. G. *Int. J. Environ. Anal. Chem.* **1995**, *59*, 225.
- (4) Borgman, U. In *Aquatic Toxicology*; Nriagu, J. O., Ed.; Wiley: New York, 1983.
- (5) Pickering, W. F. *CRC Crit. Rev. Anal. Chem.* **1981**, *12*, 233.

- (6) Tercier, M.-L.; Buffle, J. *Electroanalysis* **1993**, *5*, 187.
- (7) Tercier-Waeber, M.-L.; Belmont-Hebert, C.; Buffle, J. *Environ. Sci. Technol.* **1998**, *32*, 1515.
- (8) Belmont-Hebert, C.; Tercier, M.-L.; Buffle, J.; Fiaccabrino, G. C.; de Rooij, N. F.; Koudelka-Hep, M. *Anal. Chem.* **1998**, *70*, 2949.
- (9) Herdan, J.; Feeney, R.; Kounaves, S. P.; Flannery, A. F.; Stormont, C. W.; Kovacs, G. T. A.; Darling, R. B. *Environ. Sci. Technol.* **1998**, *32*, 131.
- (10) Wang, J.; Zadeii, J. M. *J. Electroanal. Chem.*, **1988**, *246*, 297.
- (11) Bond, A. M.; Lay, P. A. *J. Electroanal. Chem.* **1986**, *199*, 285.
- (12) Meyer, H.; Drewer, H.; Gründig, B.; Cammann, K.; Kakerow, R.; Manoli, Y.; Mokwa, W.; Rospert, M. *Anal. Chem.* **1995**, *67*, 1164.
- (13) Tercier, M.-L.; Buffle, J. *Anal. Chem.* **1996**, *68*, 3670.
- (14) Tercier, M.-L.; Parthasarathy, N.; Buffle, J. *Electroanalysis* **1995**, *7*, 55.
- (15) Belmont, C.; Tercier, M.-L.; Buffle, J.; Fiaccabrino, G. C.; Koudelka-Hep, M. *Anal. Chim. Acta* **1996**, *329*, 203.
- (16) Tercier, M. L.; Buffle, J.; Graziottin, F. *Electroanalysis* **1998**, *10*, 355.
- (17) Buffle, J.; Vuilleumier, J. J.; Tercier, M.-L.; Parthasarathy, N. *Sci. Total Environ.* **1987**, *60*, 75.

The principle of GIME microelectrodes^{8,13} is based on the embedding of the microelectrode in a gel, with well-controlled thickness (100–300 μm), which constitutes a medium from which the colloidal material is excluded, but in which the small mobile species can diffuse. Voltammetry is performed in the gel, after its equilibration (during a few minutes) with the test medium. It has been demonstrated qualitatively that a large number of aquatic colloids and polymers are excluded from the gel and that mobile and colloidal species can be discriminated.^{7,8,13,16} However, it has never been shown that this type of electrode can be used to determine quantitatively the proportions of mobile and colloidal species, the binding energy of metal to colloidal material, directly in the sample, with square wave anodic stripping voltammetry (SWASV) as the only technique.

The main purpose of this paper is to demonstrate that this is feasible, simultaneously, for Cu, Pb, Cd, and Zn, and to discuss in detail the optimum operating conditions, in particular by avoiding the most important possible artifacts. These latter problems occur, in particular, when the classical approach of metal-speciation study is used, namely the titration of the sample by large test metal concentrations (with respect to natural concentrations) while recording the corresponding voltammetric peak currents. The unrealistically large metal concentrations in solution lead to several artifacts discussed in the text. One of those is the formation of Cu–Zn intermetallic compounds^{18–21} which may modify the relative peak currents and potentials of these elements with respect to those in absence of this interference. Intermetallic compound formation is an equilibrium reaction, the importance of which increases with increasing metal concentrations in Hg and is expected to increase when passing from hanging mercury drop to Hg film electrode and to Hg microelectrode.²⁰ It will also depend on metal concentration in the test sample and accumulation time. By considering the dependence of intermetallic compounds on electrode size, the use of a microelectrode is a disadvantage, but, on the other hand, trace metal concentrations in natural waters are often low. The importance of intermetallic compound formation under these conditions has not received much attention,²² and this paper reports systematic data showing under which conditions it is negligible. The application of GIME to the speciation procedure based on sample titration by metals is then discussed. Although GIME helps the easy recording of metal-titration curves, other artifacts linked to high metal concentration levels drastically limit the use of this speciation procedure. The paper then shows how it is possible to make use of the characteristics of GIME to develop new procedures giving information on colloidal vs mobile metal fraction distribution, as well as dissociation rate and binding energy of colloidal metal, at a natural or close to natural total metal concentration level. The purpose of this paper is not to determine values of metal binding constants with specific complexants, but to show how GIME can be used to perform this type of analysis while avoiding artifacts.

EXPERIMENTAL SECTION

Chemicals. All reagents used, except $\text{Hg}(\text{CH}_3\text{COO})_2$ and KSCN (analytical-grade), were suprapur–grade. The LGL agarose

(maximum sulfur, 0.03%; gel strength at 1.5%, 2000 g cm^{-2}) was purchased from Biofinex–Switzerland. Stock solutions of Zn(II), Cd(II), Pb(II), and Cu(II) (concentration of 1 g L^{-1}) ($\text{pH} = 2$) were purchased from Merck. All solutions were freshly prepared before use by direct dilution using Milli-Q water. All the experiments were carried out at room temperature.

Fabrication of Gel-Integrated Microelectrode Arrays. The microelectrode arrays were prepared from standard silicon wafers as described in refs 8 and 15. It consisted of 5×20 Ir microdisk electrodes of 5 μm diameter with center to center spacing of 150 μm . The microelectrode arrays were prepared on a silicon wafer which was first isolated by 2000 Å LPCVD (Low-Pressure Chemical Vapor Deposition) silicon nitride, Si_3N_4 . The second step was the formation of a 2000 Å thick Ir layer by electron bombardment evaporation Ir. The Ir layer was then covered with another film of Si_3N_4 . A fourth layer made of AZ 1518 positive photoresist was deposited and developed to form a mask defining the microelectrodes and connection pad geometry. A 300- μm -thick Epon SU8 ring was deposited and patterned around the arrays of microelectrodes, forming a containment ring allowing a good attachment of agarose gel and a control of the gel thickness. The 1.8×4 mm individual devices were mounted on a Print Circuit Board, wire-bonded, and encapsulated with epoxy resin.

The Preparation of Agarose Gel Membrane. Milli-Q water was heated to about 80 °C in a water bath, and an appropriate volume of hot water was added to a known quantity of agarose placed in a test tube to obtain a gel with 1.5% agarose. The test tube was vigorously stirred, covered with a plastic wrap, reintroduced into the boiling water bath, and left in it for about 10 min after the solution began to gently boil (i.e., until all the agarose dissolves and the gel becomes transparent). The heating was stopped, and the test tube was kept in the water bath until all bubbles in the gel disappeared. Then the microelectrode array tip was dipped into the hot gel 2 or 3 times. The agarose gel on the electrode surface was left to harden in the air for about 1 min with the electrode in horizontal position and then was kept constantly hydrated. The microsensor with the protective gel must be stored in 0.1 M NaNO_3 solution when it is not in use. It is important not to leave the gel to dry in the air. The thickness of agarose gel on the top surface of the microsensor was fixed by the 300- μm -thick Epon SU8 ring deposited around the array of the microelectrodes.

The Deposition and Reoxidation of Mercury Film. Mercury films were deposited through the gel membrane before each set of experiments by maintaining the Ir potential at –400 mV (vs $\text{Ag}/\text{AgCl}/3\text{M KCl}/1\text{M NaNO}_3$) in a deoxygenated solution of 5 mM $\text{Hg}(\text{CH}_3\text{COO})_2$ and 0.1 M HClO_4 . After use, the mercury droplets were removed from the iridium substrate by reoxidation in 1 M KSCN by sweeping the potential from –300 to +300 mV at a scan rate of 5 mV/s. Both the reduction and reoxidation currents were recorded, and the radii of the mercury semidrops were determined from the corresponding electric charges.^{8,13} It has been shown that, using a Hg deposition time of 5–6 min, the Hg semidrops formed on the gel-integrated Ir-based microelectrode arrays have a spherical geometry.⁸

Instrumentation and Experimental Conditions. Electrochemical measurements were performed on a computer-controlled Amel 433A polarograph coupled to a homemade preamplifier^{14,16}

(18) Kemula, W.; Galus, Z.; Kublic, Z. *Nature (London)* **1958**, 182, 1228.

(19) Lazar, B.; Nishri, A.; Ben-Yaakov, S. *J. Electroanal. Chem.* **1981**, 125, 295.

(20) Piccardi, G.; Udisti, R. *Anal. Chim. Acta* **1987**, 202, 151.

(21) Jagner, D. *Anal. Chem.* **1978**, 50, 1924.

(22) Golimowski, J.; Szczepanska, T. *Fresenius' J. Anal. Chem.* **1996**, 354, 735.

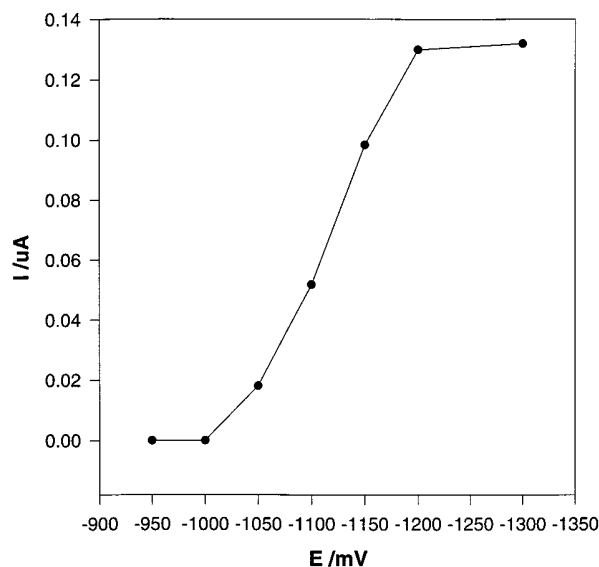


Figure 1. The effect of deposition potential on the stripping peak current of 8 nM Zn(II) in 0.1 M NaNO₃ solution. Hg diameter: 12.7 μ m. The SWASV conditions used: deposition E, -1200 mV; deposition time, 10 min; final E, 100 mV; pulse amplitude, 25 mV; step amplitude, 8 mV; wave period, 20 ms; cleaning E, 100 mV; and cleaning time, 60 s.

set at a value of 100. A three-electrode system was used, i.e., a Metrohm Ag/AgCl/3 M KCl//1 M NaNO₃ reference electrode, a Metrohm platinum rod counter electrode, and the working sensor described above. The measurement of metal concentrations in deoxygenated 0.1 M NaNO₃ solution was performed by using square wave anodic stripping voltammetry (SWASV) in the following conditions: deposition potential, -1200 mV or -1100 mV; deposition time, 10 min in quiescent solution; final potential, 100 mV; pulse amplitude, 25 mV; step amplitude, 8 mV; wave period 20 ms; sampling time, 4 ms; cleaning potential, 100 mV; and cleaning time, 60 s. A cleaning step was applied before each measurement to ensure uniform spreading of mercury layer on the iridium surface and complete removal of the elements preconcentrated in the mercury film during the previous measurement.¹⁴ It was also checked previously¹⁵ that, under the conditions used, spherical diffusion occurs around each microelectrode. Calculation shows that, for a deposition time of 10 min, overlap of the diffusion layers is negligible for a spacing of 200 μ m, which corresponds to a diffusion layer thickness of \sim 100 μ m. Thus, the diffusion layer thickness on each electrode surface is smaller than the gel thickness (300 μ m) which ensures that diffusion of species from the external solution does not influence the voltammetric peaks.

The composition in major ions of the Arve samples is given in the legend of Figure 8 and in refs 23, and 24. The samples were collected in polyethylene bottles with PTFE screw caps. Each sample was filtered through a 0.2 μ m pore size filter (NC 20 membrane filter D-37582, Dassel, Germany) just after sampling. The pHs of the samples were fixed in the following ways. In the range of pH 6.5–8, the pH was fixed by the natural HCO₃⁻ concentration and by the bubbling of a mixture of N₂ and CO₂

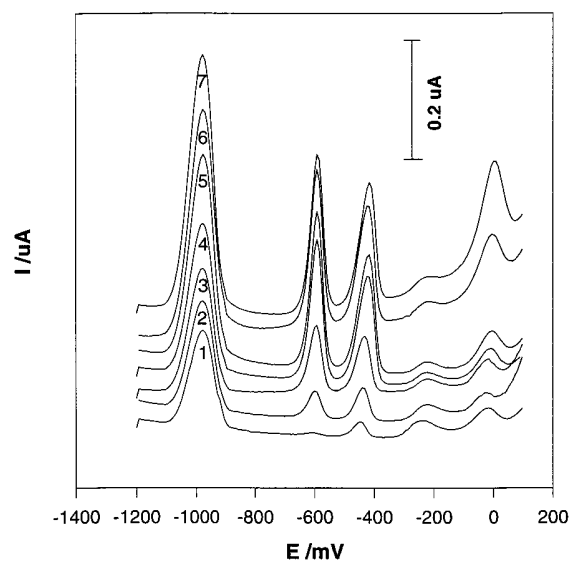


Figure 2. Successive standard additions in the filtered Arve River sample. (1) Raw water sample, pH = 7.6, Curve 2–7: river sample with following added concentrations: (2) 1 nM Pb(II), Cd(II) and 2 nM Zn(II), Cu(II); (3) 3 nM Pb(II), Cd(II), and 6 nM Cu(II), Zn(II); (4) 6 nM Pb(II), Cd(II), and 12 nM Cu(II), Zn(II); (5) 6 nM Pb(II), Cd(II) and 20 nM Cu(II) and Zn(II); (6) 6 nM Pb(II), Cd(II) and 28 nM Cu(II), Zn(II); (7) 6 nM Pb(II), Cd(II) and 36 nM Cu(II), Zn(II). Hg diameter, 12.5 μ m; SWASV conditions are the same as in Figure 1.

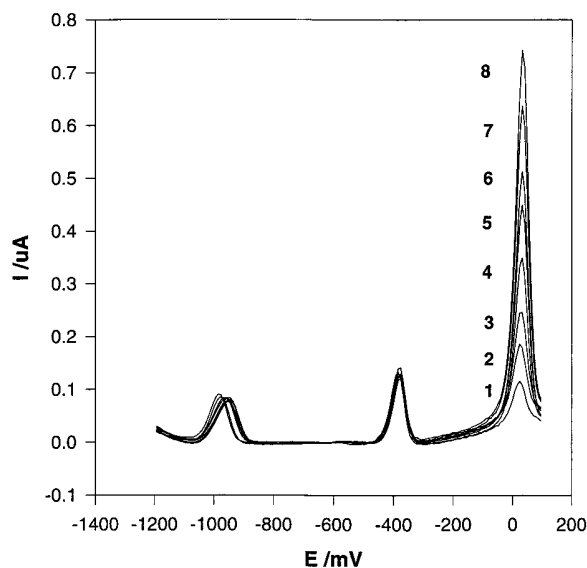


Figure 3. SWASV voltammograms of Cu(II) in 0.1 M NaNO₃ solution containing 2 nM Pb(II) and 5 nM Zn(II). Concentration of Cu(II): (1) 2, (2) 4, (3) 6, (4) 8, (5) 10, (6) 12, (7) 14, and (8) 16 nM. Hg diameter: 13.7 μ m. Other conditions are the same as in Figure 1.

gas. This latter was obtained by mixing 99.99% pure N₂ with a mixture of 5% CO₂ and 95% of 99.99% pure N₂. The pH value was fixed by the relative flow rates of the two gases and controlled automatically on-line. In the pH range 5.5–6.5, the pH value was fixed by means of 10⁻² M analytical-grade MES ((2-[N-morpholino]-ethanesulfonic acid)) buffer solutions, with pH adjusted by suprapur nitric acid and sodium hydroxide. In the pH range 4–5, the pH was fixed by means of 2 \times 10⁻² M suprapur acetate buffer solution, with pH adjusted by suprapur HNO₃ and NaOH. In the pH range 2–3.5, the pH was fixed by the right concentration of

(23) Chen, Y.; Buffle, J. *Int. J. Environ. Anal. Chem.* **1994**, 57, 125.

(24) Chen, Y.; Buffle, J. *Water Res.* **1996**, 30, 2178. (b) *Ibid.* **1996**, 30, 2185.

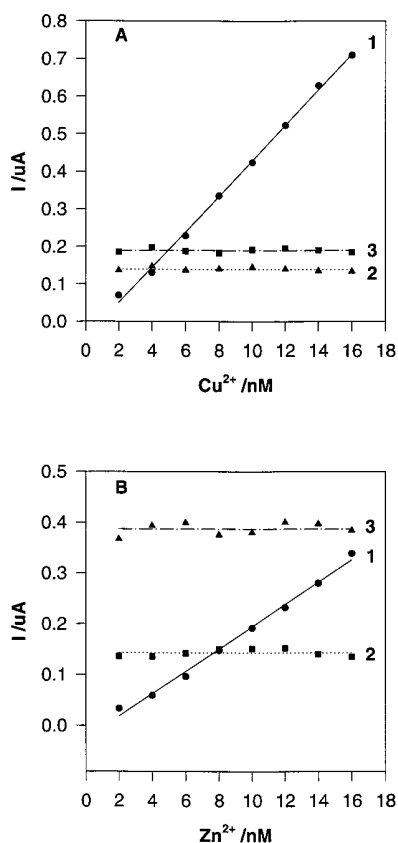


Figure 4. (A) Variations of peak currents of (1) Cu(II), (2) Pb(II) 2 nM, and (3) Zn(II) 10 nM with the added concentrations of Cu(II). Hg diameter: 13.7 μm . The slope for Cu(II) is $0.047 \pm 0.001 \mu\text{A}/\text{nM}$, $R = 0.998$ ($N = 8$) (B). Variations of peak currents of (1) Zn(II), (2) Pb(II) 2 nM, and (3) Cu(II) 10 nM to the added concentrations of Zn(II). Hg diameter: 12.7 μm . The slope for Zn(II) is $0.022 \pm 0.0007 \mu\text{A}/\text{nM}$, $R = 0.997$ ($N = 8$). Supporting electrolyte: 0.1 M NaNO_3 . Other conditions are the same as in Figure 1.

HNO_3 . A 744 pH meter (Metrohm, Switzerland) was used to monitor the value of pH. The presence of Zn(II), Cu(II), Cd(II), and Pb(II) concentrations in MES and acetate buffer were checked by blank measurements and corrected for if needed. The corrections were small or negligible compared to the Arve river release.

A voltammetric Plexiglas cell was used to minimize adsorptions and contaminations. The vessel was systematically washed by leaving it overnight with a solution of 10^{-2} M suprapur nitric acid and was reequilibrated with Milli-Q water before use. It was covered with a screwed cap. Electrolyte and acidified samples were deaerated with nitrogen gas and natural samples with the N_2 and CO_2 mixture mentioned above, for at least 10 min prior to the electrochemical measurements. A gas atmosphere was maintained over the solution during the measurements. The whole sampling and analytical procedure includes a minimum use of vessels; very careful vessel cleaning, no use of glassware; degassing with 99.99% purity gases; a minimal use of suprapur acid, base, or buffers; and very rare contact of solutions with the atmosphere. This procedure avoids contaminations or losses by adsorption. It has been used and tested in our laboratory for several years.

RESULTS AND DISCUSSION

The Tested Water Sample: Mobile vs Colloidal Metal Species. We shall discriminate below between (i) mobile metal

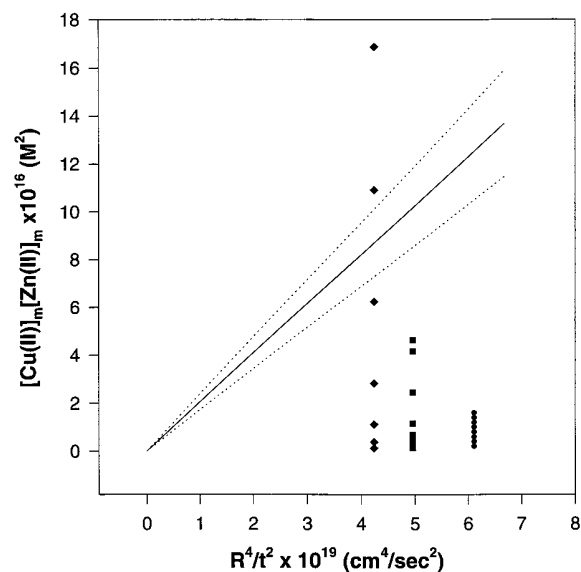


Figure 5. Limiting value of the $[\text{Cu(II)}]_{\text{m}}[\text{Zn(II)}]_{\text{m}}$ product above which intermetallic compound formation is predicted (dotted lines corresponding to the variability due to error on $K_{90} = (3.7 \pm 0.6) \times 10^{-6} \text{ M}^2$). (●): data of Figure 4A; (◆): Data of Figure 2; (■) Data of Figure 8.

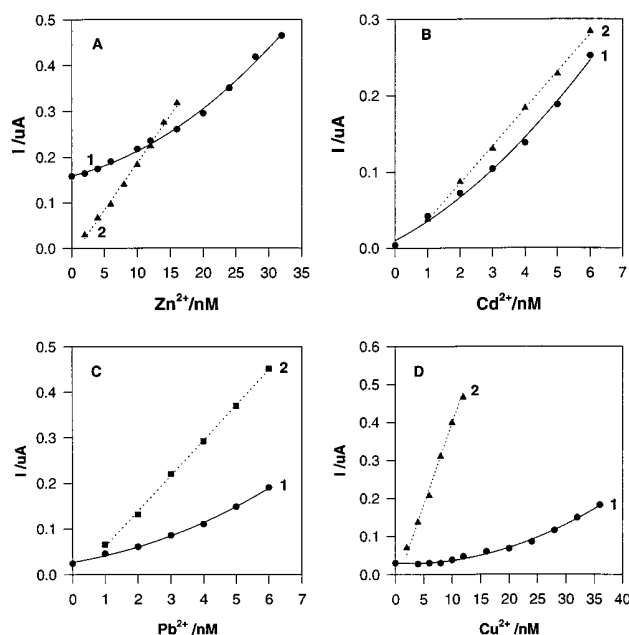


Figure 6. The relationship between the SWASV peak currents and the concentrations of (A) Zn(II), (B) Cd(II), (C) Pb(II), and (D) Cu(II) added in the Arve River sample (pH = 7.6) (Curve 1), and in 0.1 M NaNO_3 (Curve 2). Hg diameter: 13.04 μm . SWASV conditions are the same as in Figure 1.

species concentration, $[\text{M}]_{\text{m}}$, and (ii) the total metal concentration, $[\text{M}]_{\text{t}}$. The former is directly measured by GIME-SWASV, and the latter can be obtained, e.g., by AAS, ICP-MS, or GIME-SWASV, after acidification (see below). Speciation experiments have been performed on river water samples filtered on 0.20 μm pore size filters. This step was only performed to enable storage of samples for several days, for comparison purposes, as unfiltered sample composition changes very quickly through coagulation, sedimentation, and microbial activity.²⁴ It must be noted, however, that this filtration step is not required when measurements are

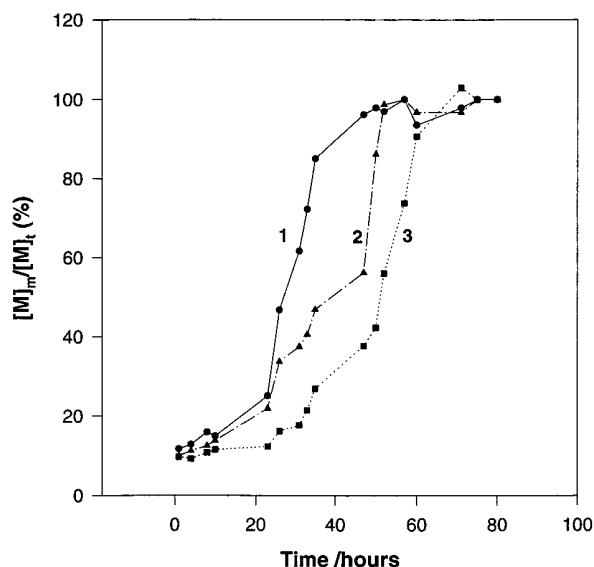


Figure 7. Kinetic of release of free metal ions from the natural complexes in Arve river sample at pH = 2.16. (1) Zn(II), (2) Pb(II), and (3) Cu(II). The SWASV conditions are the same as in Figure 1 except that deposition E is set at -1100 mV. $[M]_m$ = concentration of mobile species, $[M]_t$ = total concentration of metal.

performed in situ or on-site. Because of this step, $[M]_t$ below effectively comprises the mobile species (less than a few nanometers) and most of the colloidal fraction (a few nanometers to $1 \mu\text{m}$).

Systematic studies have already been reported for measurement of free Pb(II) and Cd(II), and their mobile species, with GIME^{8,13} and have shown that reliable, accurate response are obtained with a detection limit of 50 pM . Such a study has never been done for Cu(II) and Zn(II) and has thus been performed here. The Cu peak current was found to be independent of deposition potential in the range of -800 to -1200 mV, whereas that of Zn(II) increased significantly in the range -900 to -1200 mV (Figure 1) and reached a plateau at $E = -1200$ mV. It was found that linear current–concentration calibration curves are obtained with slopes of $47 \pm 1 \text{ nA/nM}$ and $22 \pm 0.7 \text{ nA/nM}$ for Cu and Zn respectively, in 0.1 M NaNO_3 solution, using a deposition potential of -1200 mV (see Figure 1 for other voltammetric conditions). Detection limits, based on a signal/noise ratio of 2, were 100 and 200 pM for Cu(II) and Zn(II), respectively, for a 10 min deposition time. Good linearities were also obtained for the relations between peak currents and deposition time, up to 15 min , with slopes of 40.5 and 17.3 nA/min for Cu and Zn, respectively, at 10 nM of Cu and 8 nM of Zn. A deposition time of 10 min was selected for further measurements in this paper.

Speciation of Zn(II), Cd(II), Pb(II), and Cu(II) was studied simultaneously on Arve river samples (Geneva, Switzerland, see composition in major ions in the legend of Figure 8). The Arve river contains a large load of suspended inorganic colloids and particles (mostly aluminosilicates). Typically, the annual concentration of particles varies between 50 and 100 mg/L with peaks up to 1000 mg/L and that of colloids with size $<0.8 \mu\text{m}$ varies from 2 to 3 mg/L ,^{23,24} with a large fraction of metals adsorbed on them (70 – 90% depending on the metal ion; see Table 1), resulting in low $[M]_m$ values (nanomolar to subnanomolar. See Table 1). The total organic C is low (typically 1 mg/L) and most of it is

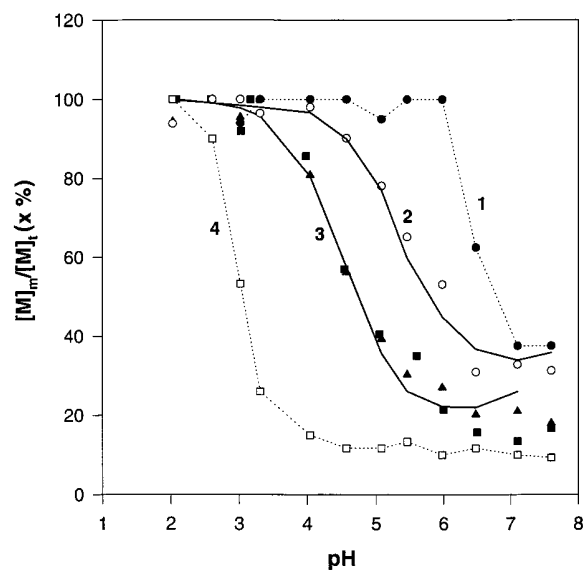


Figure 8. The effect of pH on the complexation of the metal in the Arve River. (1) Cd(II), (2) Zn(II), (3) Pb(II), and (4) Cu(II). The samples were equilibrated for more than 100 hours at each pH. Hg diameter: $13.00 \mu\text{m}$. The SWASV conditions are the same as in Figure 1. $[M]_m$ = concentration of mobile species, $[M]_t$ = total concentration of metal, see Table 1. (■) and (▲) are experimental results for Pb(II) on 2 different samples collected on May 19, 1998 and June 15, 1998, respectively. (●), (○), and (□) are experimental data for Cd(II), Zn(II), and Cu(II), respectively. Full-line curves 2 and 3 are theoretical curves for Pb(II) and Zn(II), computed from eq 18. Concentrations of the major ions and ligands (M): $[\text{Ca(II)}] 1.56 \times 10^{-3}$; $[\text{Mg(II)}] 3.0 \times 10^{-4}$; $[\text{Na}^+] 2.6 \times 10^{-4}$; $[\text{CO}_3]_{\text{tot}} 1.2 \times 10^{-3}$; $[\text{Cl}^-] 2.14 \times 10^{-4}$; $[\text{SO}_4]_{\text{tot}} 6.23 \times 10^{-4}$; $[\text{NO}_3^-] 6.6 \times 10^{-5}$; $[\text{K}^+] 3.9 \times 10^{-5}$; $[\text{Al(III)}] 5.2 \times 10^{-7}$; and $[\text{Fe(III)}] 1.11 \times 10^{-6}$; log of equilibrium constants of the complexes with Pb(II): CO_3^{2-} ($\log\beta_1 = 6.2$, $\log\beta_2 = 8.85$); OH^- ($\log\beta_1 = 6.29$, $\log\beta_2 = 10.88$, $\log\beta_3 = 13.94$); SO_4^{2-} ($\log\beta_1 = 2.75$, $\log\beta_2 = 3.47$); Cl^- ($\log\beta_1 = 1.6$, $\log\beta_2 = 1.80$, $\log\beta_3 = 1.70$, $\log\beta_4 = 1.38$); NO_3^- ($\log\beta_1 = 1.17$); HCO_3^- ($\log\beta_1 = 13.20$); and log of equilibrium constants of protonation of CO_3^{2-} ($\log\beta_1 = 10.33$, $\log\beta_2 = 16.66$).

Table 1: Voltammetric Determination of the Total Concentrations, $[M]_t$, and the Concentration of Mobile Species, $[M]_m$, of Metals in Arve River at Natural pH (7.6) at the Gel-integrated Hg-plated Ir-based Microelectrode Arrays

	$[M]_m$ (nM)	$[M]_t$ (nM) ^a	$[M]_m/[M]_t$ (%)
Zn(II)	9 ± 1	28.8 ± 3.2	31.2 ± 4.6
Cd(II)	0.1 ± 0.02	0.27 ± 0.05	37 ± 9.0
Pb(II)	0.7 ± 0.1	3.9 ± 0.6	18 ± 3.6
Cu(II)	1.5 ± 0.2	16.1 ± 2.1	9.9 ± 1.7

^a $[M]_t$ was obtained by acidification of the sample solution to pH = 2 and equilibration for 4 days.

adsorbed on particles and colloids. As a result, the mobile metal species are largely composed of aquo metal ions and inorganic metal complexes, in particular the carbonate complexes (see discussion of Figure 8), the relative proportion of the latter, however, depending on pH. They are negligibly small at $\text{pH} \leq 6$ where the aquo-ion, M^{2+} , dominates for all metals. At $\text{pH} 6$ – 7.6 , the major complexes are those formed with CO_3^{2-} , SO_4^{2-} , Cl^- , and OH^- . Their lability depends on their formation rate constants, their equilibrium constants, and also the electrode dimension.²⁵

By using the lability criteria given in ref 25, it can be checked that all these complexes can be considered as labile under the conditions used here. In addition, their diffusion coefficients are close to those of the corresponding free metal ions. In the following, all mobile complexes will then be considered to be sufficiently labile to contribute to the voltammetric signal, and their average diffusion coefficients will be taken as equal to those of the aquo ions. In particular, under such conditions, calibration curves determined in synthetic Arve river water containing only the major ions, can be used to compute the overall concentration of the mobile metal species.

$[M]_m$ values (Table 1) were determined from voltammetric peaks measured directly in the sample, at pH = 7.6. The pH was fixed by bubbling a N_2/CO_2 gas mixture. Typical voltammograms are shown in Figure 2. $[M]_l$ values for the four metals (Table 1) were obtained by voltammetric measurements on the acidified samples to pH = 2 (as discussed below).

Simultaneous Determination of Cu(II) and Zn(II) in Mixed Solutions. The importance of intermetallic Cu–Zn formation has been studied with 0.1M $NaNO_3$ solution, containing also Pb(II). This latter does not form intermetallic compounds and was used to check that any change in current or potential was due to Cu–Zn complex formation and not to a change of the electrode surface. A nanomolar concentration range has been used for this study, i.e., a range realistic for natural waters, but about 2 orders of magnitudes lower than that used in most previous studies.^{18–21}

Figure 3 shows SWASV peaks in 0.1 M $NaNO_3$ solutions containing 2 nM Pb, 5 nM Zn, and increasing concentrations of Cu(II) (2–16 nM). The peak currents of Pb(II) and Zn(II) are constant and that of Cu(II) increases linearly, as expected in absence of Cu–Zn complex formation. These behaviors show that the mercury surface is reproducible and no Cu–Zn complex is formed under these conditions. Similar curves were obtained with higher (10 nM) constant Zn(II) concentration, i.e., at larger Zn/Cu ratios in Hg electrode as shown in Figure 4A. To further confirm that no intermetallic compound is formed in the amalgam, a deposition potential of –800 mV was selected in the same solution. At this potential, only Cu and Pb (no Zn) can be deposited. The comparison of Cu peak currents deposited at –800 mV and –1200 mV did not show any significant difference and confirmed that no intermetallic compound is formed. A slight variation of Zn peak potential can, however, be seen in Figure 3, when Cu concentration increases. This is attributed to the slight pH change which occurred with increasing Cu concentrations due to the acidic pH of the Cu(II) stock solution or, more likely, to the influence of amalgam composition on Zn(0) reoxidation, since the couple Zn(II)/Zn(0) is not a fully reversible system.²⁶

Possible formation of intermetallic compounds was also checked by maintaining the concentrations of Pb(II) 2 nM and Cu(II) 10 nM constant and varying the concentration of Zn(II) (2–16 nM) (Figure 4B). Again, the peak currents of Pb(II) and Cu(II) did not change significantly with added Zn(II), whereas, that of Zn(II) increased linearly. The same results were obtained at a lower concentration of Cu(II) (5 nM instead of 10 nM).

A number of investigators have attempted to estimate the stoichiometry of the Cu–Zn intermetallic compound and to

calculate its solubility or formation constant.^{27,28} They concluded that the stoichiometry was 1:1 and, by assuming a priori that the compound in mercury was insoluble, they calculated a solubility product of $K_{so} = (3.7 \pm 0.6) \times 10^{-6} M^2$.²⁸ $CuZn_x$ ($x = 1–3$) soluble compounds have also been reported at high Cu and Zn amalgam concentrations,²⁷ but no quantitative data have been published until now. Because of the very low metal concentrations used in this study, only the 1:1 intermetallic compound is considered below. Literature results^{13,15} also show that spherical diffusion occurs at GIME electrodes, so that the number of moles of metal, N , accumulated in the amalgam during the preconcentration step follows eq 1.²⁹

$$\frac{dN}{dt} = 4\pi DC_m R \quad (1)$$

where R is the electrode radius, D the diffusion coefficient of the metal in the amalgam, t the preconcentration time, and C_m the concentration of mobile metal species in the test solution.

By integrating eq 1 and combining it with the volume of a spherical Hg microelectrode ($4\pi R^3/3$), the concentration of metal (e.g., Cu) in the amalgam $[Cu(Hg)]$ at preconcentration time t is given by:

$$[Cu(Hg)] = \frac{3D_{Cu}[Cu(II)]_m t}{R^2} \quad (2)$$

The concentration of Zn in the amalgam $[Zn(Hg)]$ is given by the same equation when both metals are reduced, so that, the metal concentration product in Hg is given by:

$$[Cu(Hg)][Zn(Hg)] = \frac{9D_{Cu}D_{Zn}t^2}{R^4} [Cu(II)]_m [Zn(II)]_m \quad (3)$$

where D_{Cu} and D_{Zn} are the diffusion coefficients of Cu^0 and Zn^0 in Hg.

The formation of the Cu–Zn intermetallic compound is expected when $[Cu(Hg)][Zn(Hg)] > K_{so}$ (where K_{so} is the corresponding solubility product), i.e., when

$$[Cu(II)]_m [Zn(II)]_m \geq \frac{K_{so}}{9D_{Cu}D_{Zn}} \frac{R^4}{t^2} \quad (4)$$

The values of the diffusion coefficients of Zn and Cu in Hg are $1.06 \times 10^{-5} cm^2 s^{-1}$ and $1.89 \times 10^{-5} cm^2 s^{-1}$, respectively,³⁰ and $K_{so} = (3.7 \pm 0.6) \times 10^{-6} M^2$.²⁸ Figure 5 shows the value of the right-hand side of eq 4, with the corresponding variability due to the error on K_{so} value. Only for ionic products larger than this limiting curve, the formation of intermetallic Cu–Zn compound is expected to be formed. Figure 5 also shows the range of ionic products corresponding to Figure 4A (●), Figure 2 (◆), and Figure 8 (■). Figure 5 confirms that no intermetallic compounds

(27) Shuman, M. S.; Woodward, G. P., Jr. *Anal. Chem.* **1976**, *48*, 1979.

(28) Rodgers, R. S.; Meites, L. *J. Electroanal. Chem.* **1981**, *125*, 167.

(29) Wightmann, R. M.; Wipf, D. O. In *Electroanalytical Chemistry*; Bard, A. J., Ed.; Marcel Dekker: New York, 1989; Vol. 15.

(30) Galus, Z. *Pure & Appl. Chem.* **1984**, *56*, 635.

(25) Leeuwen, H. P.; Pinheiro, J. P. *J. Electroanal. Chem.* **1999**, *471*, 55.

(26) Heyrovský, J. *Principles of Polarography*; Publishing House of the Czechoslovak Academy of Science: Prague, 1965.

should be formed under conditions of Figure 4A and 4B (as observed), as well as those of Table 1 and Figure 8. On the other hand, Figure 5 also confirms that intermetallic compounds may have formed for curves 6 and 7 of Figure 2, as it is experimentally observed. Thus, these results show that: (1) eq 4 is a useful prediction of intermetallic compound formation in micro (spherical) electrodes; (2) this formation can be minimized by decreasing t , provided metal concentration is not too low; (3) this formation is very sensitive to the electrode size R . To minimize intermetallic compound formation, R should be as large as possible. On the other hand, R should be as small as possible to get purely spherical diffusion, i.e., to get rid of the convective effect of the test sample. A major advantage of gel-integrated microelectrodes is that these convective effects are eliminated by the gel, so that larger size electrodes can be used in helping to minimize the intermetallic compound formation. For instance, a convenient diameter of electrode in GIME is thus 12–20 μm when intermetallic compounds are concerned, whereas without gel, a size typically $<1 \mu\text{m}$ would be necessary to avoid convection.

Complexation Studies Based on Sample Titration by Metal Ions. In literature reports, the complexation properties of natural ligands for metal ions are often extracted from so-called metal titration curves, where the water sample is titrated with the metal ion of interest, and the voltammetric signal is followed during the titration. The fraction of metal bound into electroinactive complexes (e.g., sufficiently large colloids or kinetically inert complexes) is not detected voltammetrically, and the resulting titration curve is interpreted in terms of complexation capacity (\equiv total complexing site concentration) and complexation equilibrium constant. For such a procedure, GIME presents significant advantages over other electrode types, in that: (1) it does not require the addition of electrolyte as for the conventional-size electrodes; such addition may significantly change the actual values of the complexation stability constants, and (2) it can be used directly in the water sample and left during the whole titration, without interference due to electrode fouling. Problems due to the procedure itself are, however, limiting and should be considered. It is the purpose of this section to exemplify, the intrinsic limitations of the classical procedure, how it can be used to get useful information, and the advantages of GIME for this approach, by using the results of metal titration of Arve river samples. Voltammograms of Arve river samples and of successive additions of mixtures of the four metal ions are shown in Figure 2. The relationship between peak currents and the added metal concentrations both in 0.1 M NaNO_3 and Arve River samples are shown in Figure 6 A–D. All metals show lower peak current/metal concentration ratio in the Arve River sample compared with that in 0.1 M NaNO_3 solution and display a nonlinear response indicative of metal complexation in the Arve River. The decreasing differences between the initial slopes of lines in NaNO_3 and in river sample, in the sequence $\text{Cu(II)} > \text{Pb(II)} > \text{Zn(II)} > \text{Cd(II)}$, also show that the complexing strength of the Arve River for the four metals decreases in this sequence in agreement with the known general complexation properties of these metals.^{1,2}

Curves such as those of Figure 6 are often used in the literature for the determination of the so-called complexation capacity, as an estimation of total complexation site concentration, $[\text{S}]_t$, of complexant forming colloidal and inert complexes and of the corre-

sponding apparent equilibrium constant K' at the titration pH, on the basis of the extrapolation of the part of the titration curve parallel to the calibration line obtained in synthetic media. Such interpretation of complexation titration curves must, however, be done with much caution for several reasons:^{1,31} (1) The metal complexes formed with the added metal may be quite different from the natural ones due to the much larger metal concentration used. (2) A rigorous calculation of $[\text{S}]_t$ and K' values from the titration curves is only possible when voltammetrically inert complexes, or complexes with diffusion coefficients much lower than that of the free metal ion, are formed, which is rarely the case in conditions of ligand saturation and cannot be checked easily for the whole metal titration curve. (3) The part of the titration curve parallel to the calibration line corresponds to metal concentrations much larger (sometimes by orders of magnitude) than the natural ones, where precipitation of metal ions as hydroxide or carbonate may occur and where the Cu–Zn intermetallic compound also forms. This is clearly seen on Figure 6 where the linear parts would be reached at concentrations larger than 50–100 nM for Zn(II) and Cu(II), i.e., well above Cu–Zn intermetallic compound formation (see Figures 2 and 5, and the discussion of the section on intermetallic compounds). Correct interpretation of the curves at larger metal concentrations is thus very difficult in practice. (4) Interpretations of data from titration curves are usually based on the assumption that solution contains only one complexable metal ion (M) (i.e., metal competition is not considered) and one kind of complexing site, S ,³² even though these conditions are usually not fulfilled in natural waters. In particular, they contain chemically heterogeneous complexants whose complexation properties should be represented by distribution functions of K' and $[\text{S}]_t$ values.¹ In other words, single K' and $[\text{S}]_t$ values are only valid in a restricted domain of total metal concentration, in particular, the natural one.

Useful information can be obtained from metal titration curves, only by using the data at the very beginning of the curve, in conditions where $[\text{M}]_a/[\text{M}]_t$ is small ($[\text{M}]_a$ = added metal concentration). In such conditions, all the aforementioned artifacts are minimized or eliminated. In particular, the added metals are complexed by the same ligands or complexing sites as those which are effective in natural conditions and intermetallic compounds do not form. In addition, if the range of added metal is small enough, the assumption of metal complexation by only one site type is reasonable, as well as the simultaneous determination of complexation properties for several metals, since the additional complexing site occupation by the added metals is small. Working under these conditions is possible on GIME thanks to its combined high sensitivity and enhanced reproducibility linked to the protective gel.

In this approach, an apparent complexation constant, K' , for the metal complexation by the complexing site, S , of colloids, valid at the natural metal/site ratio, pH, and composition of major ions, can be written as:

$$K' = \frac{[\text{MS}]}{[\text{M}][\text{S}']} \quad (5)$$

where $[\text{S}']$ is the sum of concentrations of the protonated or

(31) Leeuwen, H. V.; Cleven, R.; Buffle, J. *Pure Appl. Chem.* **1989**, *61*, 255.

(32) Ruzic, I. *Anal. Chim. Acta* **1982**, *140*, 99.

Table 2: Complexation Parameters Obtained for Pb(II) and Zn(II) from Metal and pH Titration

	Pb(II)	Zn(II)
metal titration		
$K'[S]_t$	25.8 ± 1.4	7.3 ± 0.5
$\log K'$ (pH 7.6)	9.3 ± 0.2	7.9 ± 0.3
$[S]_t$ (nM)	12.8 ± 2.1	97 ± 15
$\log K^a$	9.3 ± 0.2	7.9 ± 0.4
pH titration		
$\log \beta_1^H$	5.4 ± 0.3	5.9 ± 0.3
$K[S]_t$	6.5 ± 0.7	2.7 ± 0.3
$\log K^b$	8.7 ± 0.2	7.4 ± 0.2

^a K is obtained from K' value at pH 7.6, after correcting for $(1 + \beta_1^H[H^+])$ where β_1^H is obtained from pH titration. ^b K is obtained from $K[S]_t$ (pH titration) and $[S]_t$ from metal titration.

not protonated sites at the given pH. In addition, the following mass balance equations are applicable

$$[S]_t = [S'] + [MS] \quad (6)$$

and

$$[M]_t = [M] + \sum [ML_i] + [MS] = [M] \alpha_L + [MS] = [M]_m + [MS] \quad (7)$$

where $[M]_m$ is the mobile metal concentration measured by voltammetry, $\alpha_L = 1 + \sum (\beta_i[L_i])$, and L_i are the ligands forming dissolved, mobile, complexes. As discussed above, in the Arve river, ML_i are also labile. α_L is a constant depending on the sample composition, provided the added metal concentration is much smaller than $\sum [L_i]$. This is the case in the Arve river sample, since the L_i 's are the major anions (see above). In such a case, α_L can be computed from the experimentally determined values of L_i and the corresponding stability constants (legend of Figure 8).

Combining eqs 5 to 7, gives:

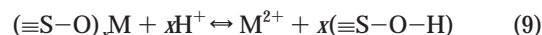
$$\frac{[M]_t}{[M]_m} - 1 = \frac{K'[S]_t}{\alpha_L} - \frac{K'}{\alpha_L}([M]_t - [M]_m) \quad (8)$$

Plotting $[M]_t/[M]_m - 1$ as function of $([M]_t - [M]_m)$ then gives a straight line, provided the metal titration range used is small enough so that the metal is complexed by one single type of site. This condition is fulfilled when $([M]_t - [M]_m)$ is not much larger than $([M]_{t,0} - [M]_{m,0})$, where the subscript 0 refers to zero added metal. Note that contrary to the assumption often used in the literature, the above condition implies that the natural total concentration of M, $[M]_{t,0}$, cannot be neglected with respect to $[M]_a$. Thus $[M]_{t,0}$ should be determined by ICPMS or voltammetry in acidified samples (see below), and $[M]_t$ in eq 8 should be computed from $[M]_t = [M]_a + [M]_{t,0}$. In such conditions, both $K'[S]_t$ and K' can, in principle, be found.

The complexation results are briefly discussed in the last section of the paper, together with the pH titration data (see also Table 2). Good estimates of K' and $[S]_t$ can be obtained for the natural ligands forming nonlabile and nonmobile complexes, at the natural metal and ligand concentrations. Similar data were

obtained by adding the metal separately rather than simultaneously. The results of Figure 6 and Table 2 emphasize that complexation titration curves are much more easily obtained with GIME than with other voltammetric electrodes, since fouling of the electrode by colloidal material does not occur. In addition, its capability of measuring the complexation of several metals simultaneously at nanomolar or even subnanomolar concentrations makes it a powerful tool for metal-competition studies. On the other hand, the interpretation of complete complexation titration curves should be done with extreme caution, due to the intrinsic problems of the procedure mentioned at the beginning of the section. Quantitative interpretation of such curves in terms of well-defined physicochemical parameters is rarely possible in natural samples and is not recommended. For this reason, the full curves of Figure 6 are not interpreted further.

Complexation Studies Based on the Dissociation of Metal Complexes, at Natural Metal Concentration: Dissociation Rate of Complexes. An alternative approach for examining the complexing properties of natural water for metals is to study the effect of pH on the corresponding voltammetric peaks. In aquatic systems, aluminosilicates (i.e., oxides of Si(IV) and Al(III)), FeOOH, and MnO₂ are major complexants, and form surface complexes with metals.^{1,2,33,34} In acidic solution, the metals are released, due to the shift of reaction 9 to the right



where M is the test metal ion, $(\equiv S-O)_xM$ is the surface metal complex, and $\equiv S-O-H$ is the surface complexing site on oxide or oxyhydroxide inorganic complexants ($x = 1$ or 2).

The complexing properties of the water sample can be measured by following the competition reaction between M^{2+} and H^+ by means of voltammetry and GIME. There are several advantages to this approach compared with that based on complete metal titration: (1) natural metal complexes are specifically studied; (2) since the study can be entirely carried out at the low (natural) metal concentration, precipitation of hydroxides or carbonates and the formation of Cu-Zn intermetallic compounds are negligible; (3) the release of several metals can be determined simultaneously in the same solution in one scan.

To get thermodynamic equilibrium constants between metals and complexing sites by this approach however, the kinetic of dissociation of metal complexes (equation 9) must be known, to ensure that equilibrium is reached at each studied pH. This is readily performed with voltammetry and GIME, since the electrode can be left in the solution to follow in real time the increase of mobile metals liberated by eq 9 (Figure 7). Classical separation techniques such as ultrafiltration or ultracentrifugation do not allow to record the details of such kinetic curves, because, in addition to the ubiquitous contamination problem at these concentrations, the separation step is too slow compared to the studied kinetic. Figure 7 shows as examples the release of Zn(II), Pb(II) and Cu(II) from the natural colloids of Arve river sample acidified to pH = 2.16, as a function of time. The peak currents increase with time over a period of 1–4 days, which

(33) Dousma, J.; de Bruyn, P. L. *J. Colloid Interface Sci.* **1976**, *56*, 527.

(34) Stumm, W. *Chemistry of the Solid-Water Interface*; Wiley: NY, 1992.

means that the ratio between mobile and total concentration ($[M]_m/[M]_t$) increases with time. Figure 7 shows that equilibrium is reached after 50 h for Zn(II) and Pb(II) and after about 60 h for Cu(II) which corresponds to the increasing order of metal-complex stabilities. A similar time was found necessary to reach equilibrium at pH 4.5, for Zn(II) and Pb(II). At this pH no Cu(II) is released (see Figure 8). Note that such detailed kinetic curves have never been reported until now in the literature for nanometer-size colloids. These rates are too slow to be explained by a slow chemical dissociation of complexes formed at the surface of the particles.³⁴ Although systematic study of dissolution of nanometer-size colloids at low concentration is difficult and far beyond the scope of this paper, it seems that this process is not significantly related to metal release. Indeed, after 4 days at pH 2, the dissolved concentrations of the major elements of colloids, Fe, Mn, and Si, measured by ICPMS, were 52 $\mu\text{g/L}$, 9 $\mu\text{g/L}$, and 65 $\mu\text{g/L}$ which must be compared with a total concentration of 4 mg/L of colloids. Above all, the fact that the release rate is similar at pH 2 and pH 4.5 strongly suggests that the metal release is not controlled by proton concentration as would be the case for dissolution of most minerals. This is in agreement with the fact that aluminosilicate particles, which constitute most minerals in the Arve river, are little soluble.²³ More likely, metals are complexed in the pores of inorganic colloids and diffusion restricted by complexation, inside these particles, is the limiting step. At any rate, these results show that the complexes dissociate very slowly and can be considered as fully inert voltammetrically. This is a key result not only for voltammetric but also for environmental interpretation of data, as metal-complex dissociation by acid is often assumed to be very fast in environmental analytical procedure, although this assumption is rarely checked.

Complexation Studies Based on the Dissociation of Metal Complexes, at Natural Metal Concentration: Proportions and Binding Energies of Metal-Colloid Complexes. The above results suggest that, in the Arve river, the release of metals by acid is a competition reaction between H^+ and M^{2+} inside and at the surface of particles (eq 9). The binding energy of metal ions to natural complexants can thus be found from an acid-base titration of the test water by measuring the proportion of mobile complexes as a function of pH. Direct voltammetry on GIME is well-suited for this measurement, as the signal is selective to mobile metal species irrespective of the concentration of colloidal, nonmobile species. The effect of pH on the complexation strength of the four metals in the Arve River was carried out in the following way: the Arve River samples filtered on a 0.2- μm filter were buffered to different pH values, spanning from pH = 2 to pH = 8, and the solutions were kept at room temperature for 4 days, allowing complete reequilibration at that pH. Then SWASV measurements were carried out, and the ratio ($[M]_m/[M]_t$) between the mobile metal species (eq 7 for definition) and the total metal concentration was plotted as a function of pH (Figure 8). The pH for half decomplexation, $\text{pH}_{1/2}$, on the pH axis is representative of the binding energy difference between M^{2+} and H^+ by natural colloids. It decreases when the binding energy of M^{2+} increases. Experimentally, it is indeed found that $\text{pH}_{1/2}$ decreases in the order $\text{Cd(II)} < \text{Zn(II)} < \text{Pb(II)} < \text{Cu(II)}$ as expected from known general complexation properties of these metals. In addition, at the river water pH, the ratio of mobile to

total metal species concentration increases in the order $\text{Cu(II)} < \text{Pb(II)} < \text{Zn(II)} < \text{Cd(II)}$ (Figure 8), which is also in agreement with the same order of binding energies.

A more quantitative interpretation can be given to the results of Figure 8. The surface complexation reaction of metal ion M and the protonation reaction of surface complexing sites can be written as follows:



The equation constant K for the complexation reaction 10 is given by eq 13

$$K = \frac{[\text{MS}]}{[\text{M}^{2+}][\text{S}]} \quad (13)$$

where $[\text{M}^{2+}]$ and $[\text{S}]$ are the free concentrations of metal ions and colloid surface sites, respectively. Note that K is the intrinsic equilibrium constant and differs from the apparent value, K' (eq 5), which is pH dependent. The mass balance equations for $[\text{M}]_t$ and $[\text{S}]_t$ are given by eqs 7 and 14 respectively:

$$[\text{S}]_t = [\text{S}] + [\text{SH}] + [\text{SH}_2] + [\text{MS}] \quad (14)$$

By combining eqs 7 and 13, one gets

$$\frac{[\text{S}]_t - [\text{M}]_t + [\text{M}]_m}{[\text{S}]} = 1 + \beta_1^{\text{H}}[\text{H}^+] + \beta_2^{\text{H}}[\text{H}^+]^2 \quad (15)$$

where β_1^{H} and β_2^{H} are the acid-base constants of the surface sites. In addition, the mobile species are composed mostly of complexes with inorganic ligands, since the dissolved fulvic compounds are negligible (see above). They can be related to the corresponding equilibrium constants (β_i) and ligand concentration $[\text{L}_i]$ by eq 16

$$\frac{[\text{M}]_m}{[\text{M}^{2+}]} = 1 + \sum_i \beta_i [\text{L}_i] = \alpha_L \quad (16)$$

By combining eqs 13, 7, 15, and 16, we can get eq 17

$$\log \left[\left(\frac{[\text{M}]_t}{[\text{M}]_m} - 1 \right) \cdot \alpha_L \right] = \log [K([\text{S}]_t - [\text{M}]_t + [\text{M}]_m)] - \log(1 + \beta_1^{\text{H}}[\text{H}^+] + \beta_2^{\text{H}}[\text{H}^+]^2) \quad (17)$$

Since α_L corresponds only to the complexation of M(II) by the simple inorganic ligands (OH^- , Cl^- , NO_3^- , SO_4^{2-} , CO_3^{2-}), its values can be computed for each of the 4 tested metals at different pH by MINTEQA2 software, using the values of stability constants given in the legends of Figure 8 and the concentrations of major inorganic ligands and ions determined experimentally (see legends of Figure 8).

Equation 17 can be used to compute the parameters K , $[S]_t$, β_1^H , and β_2^H by curve-fitting. The number of fitted parameters is large but can be reduced, in particular when $[S]_t$ is much larger than $[M]_t - [M]_m$. This condition is the more valid as pH decreases. In such a case, $K[S]_t$ can be fitted as a single parameter (eq 18):

$$\log\left[\left(\frac{[M]_t}{[M]_m} - 1\right) \cdot \alpha\right] = \log(K[S]_t) - \log(1 + \beta_1^H[H^+] + \beta_2^H[H^+]^2) \quad (18)$$

In addition, in many cases, only one acid–base constant plays an important role in the pH range of interest and it can be found from eq 18, by plotting $\log\left[\left(\frac{[M]_t}{[M]_m} - 1\right) \alpha_L\right]$ versus pH in the region of $pH_{1/2}$. For the data of Figure 8, straight lines are obtained with slopes of 1.9 for Cu(II), 0.91 for Pb(II), 0.73 for Zn(II), and 0.95 for Cd(II), respectively. This means that $\beta_2^H[H^+]^2$ is the dominant factor in the second log term of the right-hand side of eqs 17, and 18 for Cu(II), while the term $1 + \beta_1^H[H^+]$ must be considered for Pb(II), Cd(II), and Zn(II). Curves of the type of Figure 8 can then be fitted with eq 18 to find $K[S]_t$ and either β_1^H or β_2^H depending on the metal ion. Refinement is then possible by using the full eq 17. $K[S]_t$ and β_1^H parameters were computed from eq 18 (assuming $\beta_2^H[H^+]^2 = 0$) for Pb(II) and Zn(II). Values are given in Table 2, and the theoretical curves using these parameters are given as full line curves in Figure 8.

Comparison of the Complexation Data Obtained by Metal and pH Titration Methods. The complexation data obtained by both methods are summarized in Table 2, and the corresponding theoretical curves (full line curves) are compared with experimental results (symbols) in Figure 8 for Pb and Zn. Computation of K and $[S]_t$ parameters were not attempted for Cu(II) and Cd(II). In the first case, complexes are very stable. Significant error may then arise due to the very low initial slope of the metal titration curve (Figure 6) and the fact that metal release occurs at very low pH (Figure 8), where dissolution of particles might be nonnegligible. For Cd, the total concentration level was very low, which leads to high dispersion of points in Figure 8 and large errors in the fitted parameters. In addition, Figure 6 shows that significant occupation of colloidal complexing sites occurs even near the beginning of Cd(II) titration, so that $M_t - M_m$ is never small with respect to $M_{t0} - M_{m0}$ under the conditions used. These conditions may be optimized, but this was not the goal of the present work.

The theoretical curves for Pb(II) and Zn(II) in Figure 8 fit the experimental data well. Log K values obtained from metal and pH titrations are in good agreement with each other within experimental errors, both for Pb and Zn. Comparison of the data obtained by metal and pH titrations shows that they are complementary. Metal titration provides $[S]_t$ but only an apparent K' value, valid at the titration pH, whereas the pH titration provides the acid–base constant required to relate K and K' . On the other hand, determination of $[S]_t$ values from pH titration requires a large set of precise data, due to the fact that 3 parameters should be fitted. Therefore the approximate eq 18 was used in our case (with $\beta_2^H = 0$), with $K[S]_t$ and β_1^H as fitting parameters. K was then computed using the value of $[S]_t$ determined by metal titration, while the K value for metal titration was computed from

K' and the value of β_1^H from pH titration. There is a reasonable coherence of the whole set of data, within experimental errors.

Detailed comparison of the parameter values of Table 2 with literature data would require a detailed characterization of colloids since, in natural waters, clay particles may be coated by thin layers of iron oxyhydroxides or large-molecular-weight natural organic matter. This is a complicated work far beyond the scope of this paper. In addition, literature values of acid–base and complexation constants of inorganic colloids may vary by orders of magnitudes depending, in particular, on the crystalline nature of the particles. For approximate comparison, log K values for Si–OH/SiO[−], FeOH₂⁺/FeOH, and organic polyelectrolyte–COOH/COO[−] couples may vary from 5.9 to 6.8, from 5.1 to 6.1, and from 3 to 7 respectively¹. The values of 5.9 and 5.4 of Table 2 fall in this range and might be due to any of these groups. Comparison of metal complexation constants with literature data is even more difficult. Indeed, no work has been reported at these very low concentrations, and it has been clearly shown that due to the large number of site types of natural heterogeneous complexants, larger stability constants are observed at lower metal/site ratios. Log K values of Table 2 are in qualitative agreement with this observation and the few data available in the literature for higher metal/site ratios.^{1,2,34,35} Again, a complete interpretation of data would require detailed characterization and complexation studies of Arve river colloids which is beyond the scope of this paper. It clearly shows, however, that GIME is a powerful tool for such studies.

CONCLUSION

The present work describes the use of SWASV and gel-integrated Hg-plated iridium-based microelectrode arrays for simultaneous determination of Zn(II), Cd(II), Pb(II), and Cu(II) concentration and speciation measurements in an Arve River sample on the basis of its selectivity for mobile metal species. The conditions under which intermetallic compound between Cu and Zn do not form have been studied and are discussed quantitatively. It is shown that GIME presents advantages over other microelectrodes as the gel enables to work with comparatively large microelectrode on which spherical diffusion is dominant, but intermetallic compound minimized. It is also shown that the technique enables direct simultaneous determination of the proportion of metal complexes formed with colloidal complexants and the corresponding complexation parameters by competition with H⁺ or metal addition at low added metal concentrations. In addition, the release rates of the four elements in acidified (pH = 2.16) Arve River samples can also be studied at natural nanomolar or subnanomolar concentrations. They are slow and likely to be controlled by diffusion combined with complexation inside particles.

For a number of reasons, the metal titrations, with full saturation of complexing sites, by addition of metal concentrations much larger than natural ones, is not recommended. On the other hand, it is shown that useful information can be gained from minor addition of metals. This last approach may be less perturbing than pH titration when the studied colloidal particles are readily dissolved in an acidic medium. On the other hand, for acid resistant particles, the acid-titration enables to study both the

(35) Dzomfak, D. A.; Morel, F. M. M. *Surface Complexation Modeling*; Wiley: NY, 1990.

acid–base and complexation properties of complexants with the true natural complexes. In both cases, preliminary kinetic studies should be performed, to ensure that equilibrium conditions are reached, as formation/dissociation of natural complexes may be very slow (days).

Voltammetry on GIME is a unique tool for such speciation experiments, thanks to its gel layer which not only protects the electrode, but also create well-controlled and reproducible conditions in the diffusion layer at the electrode surface. These conditions, in turn, enable a high signal-to-noise ratio to be provided and an excellent reproducibility even in complicated media like surface waters, heavily loaded in colloids.

ACKNOWLEDGMENT

We acknowledge G. C. Fiaccabrino and M. Koudelka-Hep (Institute of Microtechnology, University of Neuchâtel) who have fabricated the Ir-based microelectrode arrays. This work was supported by the European Commission (Marine Science and Technology – MAST III program, contact no. MAS3-CT95-0033), as well as by funds from Swiss National Foundation.

GLOSSARY

Speciation (of Metals): There is presently no IUPAC definition of this term. In the literature it is used with different meanings, depending on the purpose and nature of the experimental work at hand. It is often used to denote detailed metal-species distribution in studies of synthetic or sufficiently simple solution, in which each metal species can be characterized. In complicated environmental samples it is most often used to denote the discrimination between groups of metal species (e.g., the whole of labile complexes, colloidal species, or complexes with natural organic matter), for which the determination of complete species distribution is not feasible. In such cases, speciation may also mean determination of equilibrium constant or complexing site concentration. The meaning of the term speciation used for complicated samples is applied in this paper.

Received for review June 11, 1999. Accepted October 13, 1999.

AC990628W